

1 **Long-term changes of nitrogen leaching and the contributions of terrestrial**  
2 **nutrient sources to lake eutrophication dynamics on the Yangtze Plain of**  
3 **China**

4 **Qi Guan<sup>a, b, c</sup>, Jing Tang<sup>d, e, \*</sup>, Lian Feng<sup>b</sup>, Stefan Olin<sup>d</sup>, Guy Schurgers<sup>c</sup>**

5 <sup>a</sup> Taihu Laboratory for Lake Ecosystem Research, State Key Laboratory of Lake Science and  
6 Environment, Nanjing Institute of Geography and Limnology, Chinese Academy of Sciences, Nanjing  
7 210008, China.

8 <sup>b</sup> School of Environmental Science and Engineering, Southern University of Science and Technology,  
9 Shenzhen 518055, Guangdong, China.

10 <sup>c</sup> Department of Geosciences and Natural Resource Management, University of Copenhagen,  
11 Copenhagen, Denmark.

12 <sup>d</sup> Department of Physical Geography and Ecosystem Science, Lund University, Lund, Sweden.

13 <sup>e</sup> Department of Biology, University of Copenhagen, Copenhagen, Denmark.

14 \* Corresponding author: [jing.tang@nateko.lu.se](mailto:jing.tang@nateko.lu.se)

15 **Abstract**

16 Over the past half-century, drastically increased chemical fertilizers have entered agricultural  
17 ecosystems to promote crop production on the Yangtze Plain, potentially enhancing agricultural nutrient  
18 sources for eutrophication in freshwater ecosystems. However, long-term trends of nitrogen dynamics  
19 in terrestrial ecosystems and their impacts on eutrophication changes in this region remain poorly  
20 studied. Using a process-based ecosystem model, we investigated the temporal and spatial patterns of  
21 nitrogen use efficiency (NUE) and nitrogen leaching on the Yangtze Plain from 1979 to 2018. The  
22 agricultural NUE for the Yangtze Plain significantly decreased from 50 % in 1979 to 25% in 2018, with  
23 the largest decline of NUE in soybean, rice and rapeseed. Simultaneously, the leached nitrogen from  
24 cropland and natural land increased with annual rates of 4.5 kg N ha<sup>-1</sup> yr<sup>-2</sup> and 0.22 kg N ha<sup>-1</sup> yr<sup>-2</sup>,  
25 respectively, leading to an overall increase of nitrogen inputs to the fifty large lakes. We further  
26 examined the correlations between terrestrial nutrient sources (i.e., the leached nitrogen, total

27 phosphorus sources, and industrial wastewater discharge) and the satellite-observed probability of  
28 eutrophication occurrence (PEO) at an annual scale, and showed that PEO was positively correlated  
29 with the changes in terrestrial nutrient sources for most lakes. Agricultural nitrogen and phosphorus  
30 sources were found to explain the PEO trends in lakes in the western and central part of the Yangtze  
31 Plain, and industrial wastewater discharge was associated with the PEO trends in eastern lakes. Our  
32 results revealed the importance of terrestrial nutrient sources for long-term changes in eutrophic status  
33 over the fifty lakes of the Yangtze Plain. This calls for region-specific sustainable nutrient management  
34 (i.e., nitrogen and phosphorus applications in agriculture and industry) to improve the water quality of  
35 lake ecosystems.

## 36 **1 Introduction**

37 For the past half-century, China's demand for grain production has increased from 250 Mt in 1960 to  
38 648 Mt in 2010 along with the growing population, industrial development, and human-diet changes  
39 (Zhao et al., 2008; Wang and Davis, 1998). Substantial chemical fertilizers (i.e., 35 mega-tons, Mt,  
40 nitrogen fertilizers in 2014 (Yu et al., 2019) simultaneously entered agricultural ecosystems for the  
41 promotion of crop production. Although national grain production consequently increased from 132 Mt  
42 in 1950 to 607 Mt in 2014 (Yu et al., 2019), such a level of fertilization has enhanced nitrogen discharge  
43 to terrestrial and freshwater ecosystems, leading to a series of ecological and environmental concerns,  
44 such as soil nitrogen pollution, water quality deterioration, and phytoplankton blooms (Zhang et al.,  
45 2019; Wang et al., 2021b; Qu and Fan, 2010). It was reported that approximately  $14.5 \text{ Mt N yr}^{-1}$  was  
46 discharged to surface water ecosystems over entire of China for the period of 2010-2014, which largely  
47 exceeded the national safe level of nitrogen discharge (i.e.,  $5.2 \text{ Mt N yr}^{-1}$ ) for the aquatic environment  
48 (Yu et al., 2019). Such human-related nutrient enrichment poses a big challenge to China's sustainable  
49 development goals (Wang et al., 2022).

50 The Yangtze Plain, with a human population of 340 million and an agricultural area of 100 million  
51 hectares (Chen et al., 2020b; Hou et al., 2020), is experiencing unprecedented ecological and  
52 environmental issues (Guan et al., 2020; Feng et al., 2019). From 1990 to 2015, total crop production  
53 increased by 15 % at the expense of an increase of 89 % in nitrogen fertilizers over the Yangtze Plain

54 (Xu et al., 2019). Consequently, more frequent nitrogen pollution was observed in soil and water. For  
55 example, heavy fertilizer usage and intensive livestock contributed to soil nitrogen pollution in the  
56 Yangtze River Delta for the past four decades, leading to soil deterioration and nitrogen discharge (Zhao  
57 et al., 2022). Nitrogen discharge related to human activities (i.e., fertilizer and manure applications, and  
58 human food waste) largely increased the nutrient loading and accelerated the degradation of water  
59 quality in the Yangtze River since the 1990s (Chen et al., 2020c). Under the recent sustainable  
60 development plans proposed by national and local governments, managing nitrogen sources from urban  
61 and crop systems is envisaged to mitigate severe soil and water pollution (Chen et al., 2020c; Zhao et  
62 al., 2022; Shi et al., 2020). However, for the Yangtze Plain with a variety of crops and crop management,  
63 the lack of insights into long-term changes in nitrogen dynamics, such as fertilizer application, plant  
64 nitrogen uptake, and nitrogen leaching, has limited our solution of proposing effective policies related  
65 to nutrient management.

66 In recent several decades, national field surveys and satellite observations have been widely used to  
67 investigate nutrient loadings (Tong et al., 2017; Li et al., 2022), chlorophyll-a concentrations (Guan et  
68 al., 2020), trophic state index (TSI) (Hu et al., 2022; Chen et al., 2020a) and algal bloom occurrence  
69 (Huang et al., 2020) to assess eutrophication issues in local or regional lakes of the Yangtze Plain, all  
70 of which revealed the lakes on the Yangtze Plain experienced eutrophication and algal blooms for the  
71 past two decades. Cyanobacteria blooms were reported to frequently occur in Taihu and Chaohu lakes,  
72 with the peak expanded extent reported for 2006 (Qin et al., 2019). Since then, the magnitudes of algal  
73 blooms significantly decreased from 2006 to 2013, and slightly increased again from 2013 to 2018  
74 (Huang et al., 2020). Satellite observations revealed widespread and serious eutrophication issues in  
75 large lakes of the Yangtze Plain for the periods of 2003-2011 and 2017-2018, although significantly  
76 decreasing trends were found in 20 out of 50 lakes throughout the periods (Guan et al., 2020). Moreover,  
77 35-year Landsat-derived trophic state index (TSI) also indicated that hyper-eutrophic and eutrophic  
78 lakes mainly characterized the Yangtze Plain, with slight increase in TSI from 1986 to 2012 and then  
79 decrease since 2012 (Hu et al., 2022). National field surveys demonstrated that although total  
80 phosphorus concentrations overall decreased from 2006 to 2014, it still remained under high levels

81 (i.e.,  $> 50 \mu\text{g L}^{-1}$ ) in eastern China lakes (Tong et al., 2017). Various laws and guidelines were  
82 implemented on regional and national scales to control eutrophication problems, such as the Guidelines  
83 on Strengthening Water Environmental Protection for Critical Lakes in 2008 and the Water Pollution  
84 Control Action Plan in 2015 (Huang et al., 2019). Nevertheless, the eutrophication issues are still  
85 challenging to control and improve under the scarcity of effective strategies for the whole Yangtze Plain  
86 due to the unknown causes of eutrophication issues.

87 To understand the primary causes of eutrophication in the lakes of the Yangtze Plain, previous studies  
88 have attempted to determine the contributions of riverine nutrient exports and lacustrine nutrient loading  
89 to algal blooms in individual lakes, such as Taihu and Chaohu lakes (Tong et al., 2017; Tong et al.,  
90 2021; Xu et al., 2015). Based on field-measured phytoplankton biomass and nutrient concentrations,  
91 algal blooms in Taihu Lake were primarily attributed to excessive nutrient loads from 1993 to 2015  
92 (Zhang et al., 2018). Overloaded nutrients, in combination with climatic warming, were found to  
93 regulate the seasonal variations of cyanobacteria blooms in Chaohu Lake based on the monthly nutrient  
94 monitoring at discrete points (Tong et al., 2021). However, these studies only tracked the primary  
95 drivers of algal blooms for individual hyper-eutrophic lakes (i.e., Taihu and Chaohu lakes), which is  
96 insufficient to understand regional variations in terms of the causes of eutrophication and support the  
97 design of effective management strategies to mitigate eutrophication issues across different eutrophic  
98 states of lakes. Furthermore, lacustrine nutrient loading is always associated with terrestrial nutrient  
99 sources, such as synthetic fertilizers, livestock manure, and industrial sewage (Wang et al., 2019b; Yu  
100 et al., 2018). For example, Wang et al. (2019b) identified that diffuse sources contributed 90% to  
101 riverine exports of total dissolved nitrogen, and point sources discharged 52% of riverine phosphorus  
102 exports to Taihu Lake, where diffuse sources are synthetic fertilizers and atmospheric deposition, and  
103 point sources are sewage and manure discharge. It was also reported that chemical fertilizer and  
104 wastewater discharge provided primary nitrogen sources for the Chaohu Lake (Yu et al., 2018).  
105 Unfortunately, all these studies did not examine the impacts of vegetation uptake and soil retention on  
106 terrestrial nutrient sources, making it insufficient to comprehensively understand the linkage between  
107 terrestrial nutrient sources and eutrophication in regional lake ecosystems.

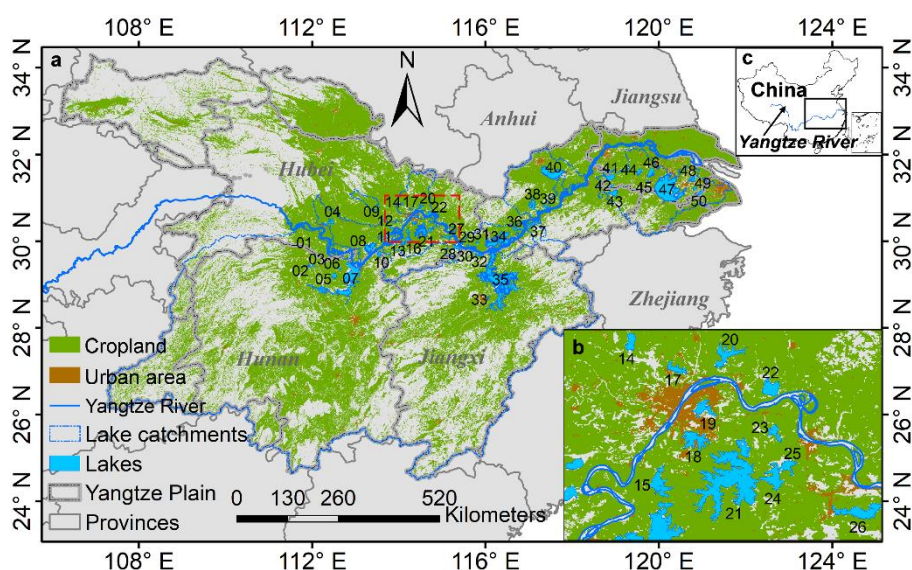
108 In this study, we employed a process-based dynamic vegetation model, LPJ-GUESS (Smith et al., 2014),  
109 to investigate terrestrial nitrogen dynamics for the past four decades, examining the primary drivers of  
110 eutrophication trends in fifty large lakes of the Yangtze Plain (covering 63% of the whole plain). We  
111 simulated the vegetation dynamics, nitrogen cycles for agricultural and natural ecosystems from 1979  
112 to 2018, and then assessed the temporal trends of nitrogen use efficiency and nitrogen leaching. The  
113 terrestrial nutrient sources were used to examine their linkage with the satellite-derived eutrophication  
114 changes for fifty large lakes.

## 115 **2 Materials and Methods**

### 116 **2.1 Study area**

117 The Yangtze Plain (Fig. 1) is in the middle and lower basin of the Yangtze River. It covers a total area  
118 of  $7.8 \times 10^6$  km<sup>2</sup> from Hunan Province to Shanghai City, and accommodates approximately 5000  
119 freshwater lakes, ponds and reservoirs (Hou et al., 2017). Its sub-tropical monsoon climate provides  
120 annual mean temperature (~15°C) and precipitation (~1000 mm) conditions favorable for crop  
121 cultivation, in particular cereals and oil seeds, making the Yangtze Plain one of the top three food  
122 production regions in China. Generally, rice-sown area contributed dominantly to agriculture areas  
123 associated with climate conditions and human diet (Piao et al., 2010; Tilman et al., 2011). To enhance  
124 crop production, double-cropping strategy has been widely implemented on the Yangtze Plain, such as  
125 the rotation of early- and late-season rice (Chen et al., 2017), and the rotation of summer maize and  
126 winter wheat (Xiao et al., 2021). Several common management practices were adopted by millions of  
127 smallholders (Cui et al., 2018). For example, straw return, organic manure applications, and suitable  
128 planting density were also recommended in recent years (Cui et al., 2018). Significantly increased  
129 fertilizer applications to cropland were expected to stimulate crop yield over the past half century (Yu  
130 et al., 2019; Zhang et al., 2015). Such management practice can certainly enhance agriculture  
131 productivity, but also cause negative consequences to soil and aquatic environment (Liu et al., 2016a;  
132 Shi et al., 2020). However, since the policy of Reform and Opening-up of China in the 1980s (Zhang  
133 et al., 2010), agricultural ecosystems have been confronted with great pressure from urban expansion

134 on the Yangtze Plain. Rapid urban expansion encroached on arable land, mainly on the eastern parts of  
135 the Yangtze Plain (Zhang et al., 2021).



136

137 **Figure 1.** Locations of the Yangtze Plain and the fifty large lakes studied here. (b) Detailed overview  
138 of Wuhan region (red box in (a)) and the surrounding lakes.

## 139 2.2 Dynamic vegetation model

140 We used a dynamic ecosystem model, LPJ-GUESS (Smith et al., 2014; Olin et al., 2015b), to simulate  
141 vegetation dynamics (i.e., the establishment, growth, competition, and mortality of plants), soil  
142 biogeochemistry, and carbon and nitrogen cycles for different ecosystems on the Yangtze Plain. The  
143 model has been widely used to assess ecosystem carbon and nitrogen fluxes at regional and global scales  
144 (Smith et al., 2014). Plant functional types (PFTs) and crop functional types (CFTs) are designed to  
145 describe the different types of plants and crops with a set of pre-defined bioclimatic and physiological  
146 parameters, such as photosynthetic pathways, phenology, growth forms and life history strategies for  
147 PFTs, as well as irrigation, fertilization, and rotation schemes for CFTs (Smith et al., 2014; Sitch et al.,  
148 2003; Olin et al., 2015a; Lindeskog et al., 2013).

149 Carbon and nitrogen fluxes between ecosystems and the atmosphere are calculated on a daily basis. For  
150 natural PFTs, net primary production (NPP) is accumulated and allocated to different plant  
151 compartments (i.e., leaves, roots, sapwood and heartwood for trees) at the end of each simulation year.

152 Soils are represented by 11 carbon and nitrogen pools with different decomposition rates (Parton et al.,  
153 1993; Parton et al., 2010), dependent on soil temperature and texture, water content, and base decay  
154 rates (Smith et al., 2014). Atmospheric deposition and plant biological fixation provide nitrogen sources  
155 for plant growth and development, while the decomposition of soil organic matter can release mineral  
156 N into the soil and nitrogen-related gases into the atmosphere. Moreover, soluble nitrogen in soil can  
157 also leach with the surface runoff in the forms of dissolved organic and inorganic nitrogen (i.e., DON  
158 and DIN). In the model, leaching of DON is a function of the decay rates of soil microbial carbon pool  
159 and soil percolation, while DIN leaching depends on the available mineral nitrogen in soils and soil  
160 percolation, as well as soil water content.

161 Crop growth starts from a seedling with initial carbon and nitrogen masses at a prescribed sowing date.  
162 Chemical fertilizer and livestock manure supply external nitrogen for crop growth. According to local  
163 farmers' practice (Shi et al., 2020), chemical fertilizer and manure applications are often applied at three  
164 different stages: sowing, tillering, and heading stages. Such fertilization schemes are also represented  
165 in the LPJ-GUESS (Olin et al., 2015a), where nitrogen fertilizer is applied when the crop development  
166 stage reaches 0, 0.5, and 0.9 in response to three above stages, and the relative fertilization rate for each  
167 stage are empirical parameters based on field surveys. Crop N uptake is simulated as the lesser between  
168 crop N demand and accessible mineral N in soils, where the former depends on crop development stages  
169 and C:N ratios of leaves and roots, and the latter is affected by soil temperature and fine root biomass  
170 (Olin et al., 2015a). Differing from natural PFTs, NPP is allocated to leaves and stems, root, and storage  
171 organs for each CFT on a daily basis, according to the daily allocation strategies related to crop  
172 development stages (Olin et al., 2015a).

## 173 **2.3 LPJ-GUESS input, calibration, and evaluation dataset**

### 174 **2.3.1 Input data**

175 We ran LPJ-GUESS separating four land use types (natural land, cropland, pasture and urban) with a  
176 500-year spin-up to simulate the vegetation dynamics and the associated nitrogen fluxes for the Yangtze  
177 Plain from 1979 to 2018.

178 The gridded input data for LPJ-GUESS include climate, fractions of four land use types, total chemical  
179 fertilizer and manure application rates, cover fractions of each CFT within the cropland area, and soil  
180 properties. We used daily temperature, precipitation, and shortwave radiation provided by the China  
181 Meteorological Forcing Dataset (CMFD), with a spatial resolution of  $0.1^\circ$  and a temporal coverage of  
182 1979-2018 (He et al., 2020). The 300-m Climate Change Initiative Land Cover (CCI-LC version 2.0)  
183 dataset was regrouped into four different land use types (i.e., urban, cropland, pasture, and natural land)  
184 to obtain the cover fractions within each  $0.1^\circ$  grid cell for the period of 1992 to 2018 (Defourny et al.,  
185 2012) (see the details about regrouping process in Supplementary S1). Soil properties, i.e., fractions of  
186 sand, clay and silt, organic carbon content, C:N, pH, and bulk density were extracted from the World  
187 Inventory of Soil Property Estimates (WISE30sec) dataset (Batjes, 2016). Based on the original data  
188 with a spatial resolution of 30 sec, we determined the dominant FAO soil type based on their relative  
189 area in each grid cell, and used its properties as input data for the grid cell. Gridded chemical fertilizer  
190 and manure application data were extracted from global fertilizer usage (Lu and Tian, 2017) and manure  
191 data (Zhang et al., 2017), which have spatial resolutions of  $0.5^\circ$  and  $0.5'$ , respectively. We resampled  
192 the fertilizer and manure application data into the spatial resolution of  $0.1^\circ$  to represent the chemical  
193 fertilizer and manure application for each grid cell from 1979 to 2014. The gridded monthly N  
194 deposition data were also extracted from an external database as an input file (Lamarque et al., 2013).  
195 It has a spatial resolution of  $0.5^\circ$ , and we used the value in the nearest grid cell to represent N deposition  
196 in the simulations.

197 The gridded fractions of CFTs were calculated based on observational data provided by the China  
198 Meteorological Data Service Center (<https://data.cma.cn/site/subjectDetail/id/101.html>). The dataset  
199 contains the information about the types, sowing and harvest dates for a total of eleven crops at 92  
200 observational sites across the whole Yangtze Plain (listed in Table S1). An adaptive inverse distance  
201 weighting method was then used to interpolate the maps of the relative fractions of all crops, and their  
202 sowing and harvest dates for the period of 1992-2015 (see the details in Supplementary S2). Due to the  
203 limited availability for the period of 1979-1991 and 2016-2018, we used the same crop information (i.e.,  
204 the fractions of crop types, sowing and harvest dates) from the nearest years.



### 205 **2.3.2 Model calibration and evaluation data**

206 The model was calibrated based on the observed crop yield collected by the China Meteorological Data  
207 Service Center (<https://data.cma.cn/site/showSubject/id/102.html>). The dataset provides crop yield data  
208 for eight main crops collected at different numbers of sites (i.e., winter wheat (number of sites: 37),  
209 spring maize (6), summer maize (10), single-season rice (28), early-season rice (30), late-season rice  
210 (30), rapeseed (38), and soybean (15)), for the period of 2000-2013. For the Yangtze Plain, hybrid and  
211 super-hybrid rice are widely cultivated to obtain high grain yield within short growing seasons due to  
212 the enhanced photosynthetic rates associated with leaf-level chlorophyll and rubisco contents (Huang  
213 et al., 2016). However, the default parameters for rice CFTs in LPJ-GUESS cannot capture the high-  
214 yield features of hybrid and super-hybrid rice. Therefore, we calibrated the relationship between the  
215 leaf-based nitrogen content and the maximum catalytic capacity of rubisco (see the details in  
216 Supplementary S3). We randomly selected five sites with rice yield data from 2000 to 2013 as the  
217 calibration data, and the other rice yield data were used as the evaluation data. For parameters of other  
218 CFTs (listed in Table S1), the default values performed satisfactorily in the comparison with all  
219 observed yield data (Fig. 2). It is noted that regional mean yield for each crop was derived from the  
220 evaluation data to compare the simulated values on the Yangtze Plain.

221 Simulated GPP and LAI were further compared with Global Solar-induced Chlorophyll Fluorescence  
222 Gross Primary Productivity (GOSIF GPP) and third generation of Global Inventory Modeling and  
223 Mapping Studies Leaf Area Index (GIMMS LAI3g) products to evaluate the performance of modelled  
224 vegetation variables. The global GOSIF GPP products have a spatial resolution of 0.05° and cover the  
225 period of 1992-2018 (Li and Xiao, 2019). Biweekly GIMMS LAI3g products with a spatial resolution  
226 of 0.25° were obtained and then converted to annual mean LAI3g maps from 1982 to 2011 (Zhu et al.,  
227 2013).

228 The modelled responses of nitrogen leaching to different fertilizer applications were evaluated based  
229 on an observational dataset published by Gao et al. (2016), where they collected nitrogen leaching for  
230 plots with 3 or 4 different levels of nitrogen fertilizer inputs for maize, rice, and wheat. In our study, we  
231 selected the observed responses without influences of phosphorus and potash fertilizers on the Yangtze

232 Plain as the evaluation data (two samples for each crop). For these sites, individual simulations were  
233 performed by assigning the full coverage of each corresponding crop growth and prescribing the levels  
234 of nitrogen fertilizer applications as in the experimental site. It should be noted that we used the same  
235 nitrogen fertilizer applications in the period prior to the field experiment.

## 236 **2.4 Assessment of long-term changes in nitrogen dynamics**

237 We assessed long-term changes in nitrogen use efficiency (NUE) and nitrogen leaching over the past  
238 four decades. For the LPJ-GUESS simulated NUE and leached nitrogen, a linear regression was  
239 conducted on the annual mean values for the whole Yangtze Plain to determine the associated change  
240 rates (i.e., the regression slopes), and the significance was tested by a *t*-test. The mean leached nitrogen  
241 over the drainage area of all examined lakes was calculated to explore long-term changes in terrestrial  
242 nitrogen sources for lake ecosystems, and the associated temporal trends were assessed by the linear  
243 regression and *t*-test.

## 244 **2.5 Examination of the primary driving forces of eutrophication dynamics**

### 245 **2.5.1 Satellite-derived eutrophication changes**

246 We used satellite-derived PEO data published in Guan et al. (2020) to represent the eutrophication  
247 changes for fifty large lakes on the Yangtze Plain. The PEO was defined as the frequency of high  
248 chlorophyll-a concentrations (i.e.,  $> 10 \text{ mg m}^{-3}$ ) or algal bloom occurrences in satellite imagery for each  
249 year. All full-resolution (300 m) MERIS and OLCI images were used to derive chlorophyll-a  
250 concentrations by using a SVR-based piecewise retrieval algorithm, and also detect algal bloom through  
251 two indices. High temporal resolutions for MERIS (i.e., 3 days) and OLCI (i.e., 1-2 days) ensure to  
252 provide sufficient observations on rapidly dynamic lake ecosystems. The averaged PEO values for  
253 pixels within each lake were then obtained to delineate the eutrophication status and changes in fifty  
254 large lakes of the Yangtze Plain during the MERIS (i.e., 2003-2011) and OLCI (i.e., 2017-2018)  
255 observational periods. However, due to the unavailability of the crop- and nitrogen-related data for the  
256 period of 2017-2018, we only used the PEO data derived from MERIS observations (i.e., 2003-2011)  
257 here to examine their primary driving forces.

## 258 **2.5.2 Examination of the correlations between nutrient and PEO anomalies**

259 To examine the impacts of terrestrial nutrient sources on eutrophication changes in fifty large lakes of  
260 the Yangtze Plain, we used the simulated nitrogen leaching (LN) and anthropogenic phosphorus sources  
261 (i.e., total phosphorus from chemical fertilizer and manure, TP) representing the agricultural nutrient  
262 sources, and industrial wastewater discharge (IW) representing industrial nutrient sources. The gridded  
263 phosphorus fertilizer data were extracted from a global dataset developed by Lu and Tian (2017), while  
264 the phosphorus content in manure was calculated based on the nitrogen contents of manure products  
265 and the associated N:P ratios of different animals' excrement (Table S3). Annual industrial wastewater  
266 discharge data were obtained from the China City Statistical Yearbook ([https://data.cnki.net/trade/Year-](https://data.cnki.net/trade/Year-book/Single/N2018050234?zcode=Z011)  
267 [book/Single/N2018050234?zcode=Z011](https://data.cnki.net/trade/Year-book/Single/N2018050234?zcode=Z011)). Note that both agricultural phosphorus sources and  
268 industrial wastewater discharge are inventory data.

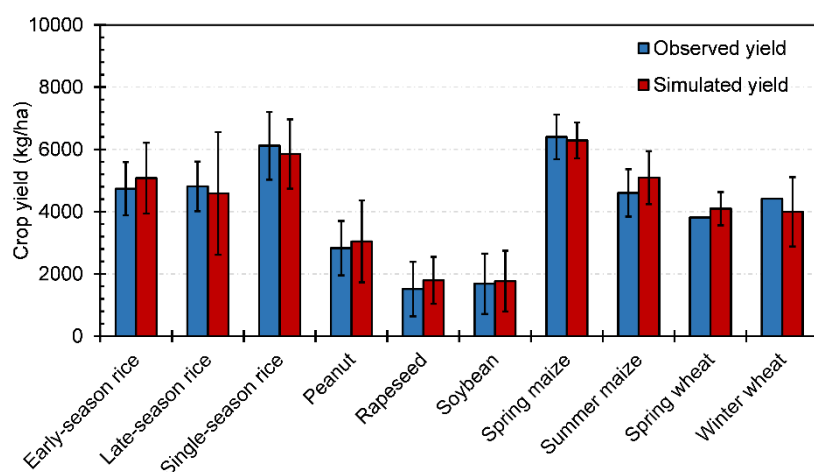
269 The 9-year mean (2003-2011) of three nutrient-related variables (i.e., LN, TP and IW) was used in a  
270 principal component analysis (PCA) followed by a K-means clustering (Hartigan and Wong, 1979) to  
271 classify examined fifty lakes based on similarities of terrestrial nutrient sources. In this process, all  
272 variables were normalized (across all years and lakes) based on the z-score method to remove the  
273 influence of different magnitudes in nutrient-related variables. We derived the first two principal  
274 components (PCs) from all normalized variables through a PCA, and the lakes were classified into three  
275 classes based on the first two PCs through the clustering methods. Finally, the annual anomalies of these  
276 nutrient-related variables and PEOs relative to their 9-year means were used to determine the primary  
277 drivers of temporal trends in eutrophication for each lake class.

## 278 **3 Results**

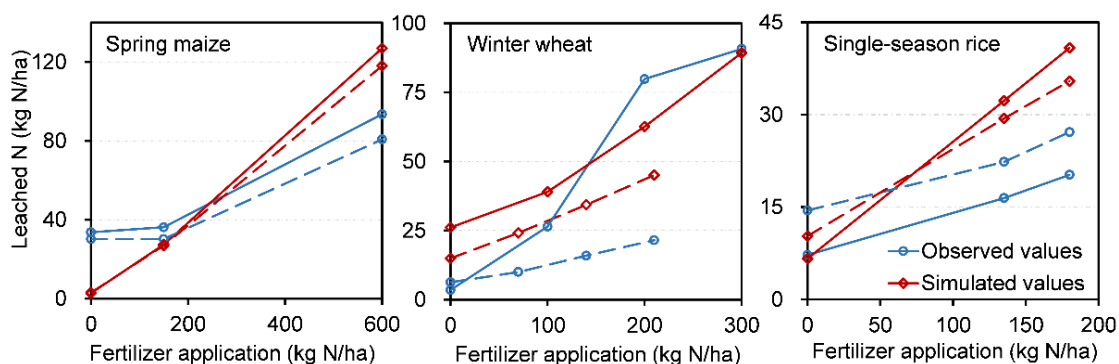
### 279 **3.1 Evaluation of LPJ-GUESS simulation**

280 For the evaluation of LPJ-GUESS simulation for the past four decades, the simulated LAI, GPP and  
281 crop yield were compared with observation-based estimates. Mean crop yields agreed well with the  
282 observed values, with mean relative errors of < 10% (Fig. 2). The comparison of simulated and observed  
283 LAI, and GPP were also satisfactory with overall high accuracy (i.e., a mean relative error of ~20% and

284 the root squared relative errors of < 30%) and spatial distributions consistent with observed patterns  
 285 (Fig. S1 and S2). Considering the difference in spatial scales between the grid cells and the gridded  
 286 evaluation data (i.e., the observed LAI and GPP maps), the overall performance of vegetation simulation  
 287 over the different land use types was considered acceptable. In addition, the simulated responses of  
 288 nitrogen leaching to different fertilizer applications at the experimental sites showed overall similar  
 289 trends as the observation ones for all three crops (i.e., maize, rice, and wheat), despite varying  
 290 magnitudes of differences between the simulated and observed leached nitrogen at certain fertilizer  
 291 level (Fig. 3).



292  
 293 **Figure 2.** Comparison between the simulated and observed crop mean yields of different crops on the  
 294 Yangtze Plain; the mean values were averaged over the period 2000-2015 and across totally 179 sites.  
 295 Error bars show one standard deviation of crop yield.



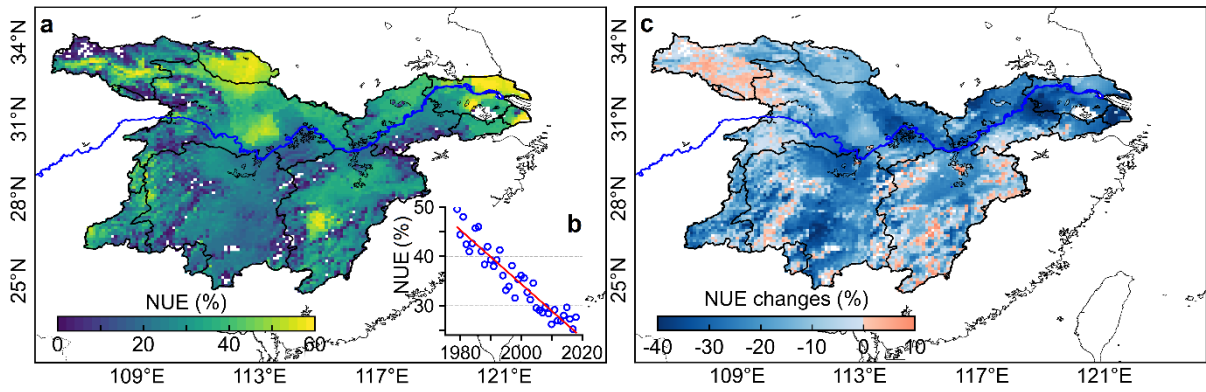
296  
 297 **Figure 3.** The simulated and observed responses of the leached nitrogen to different levels of fertilizer  
 298 application rates for three main crop types (i.e., maize, rice, and wheat) over the Yangtze Plain. Note

299 that the solid and dotted lines represented two different pairs of simulated and observed response of  
300 leached nitrogen, respectively.

### 301 **3.2 Long-term changes of nitrogen use efficiency over the Yangtze Plain**

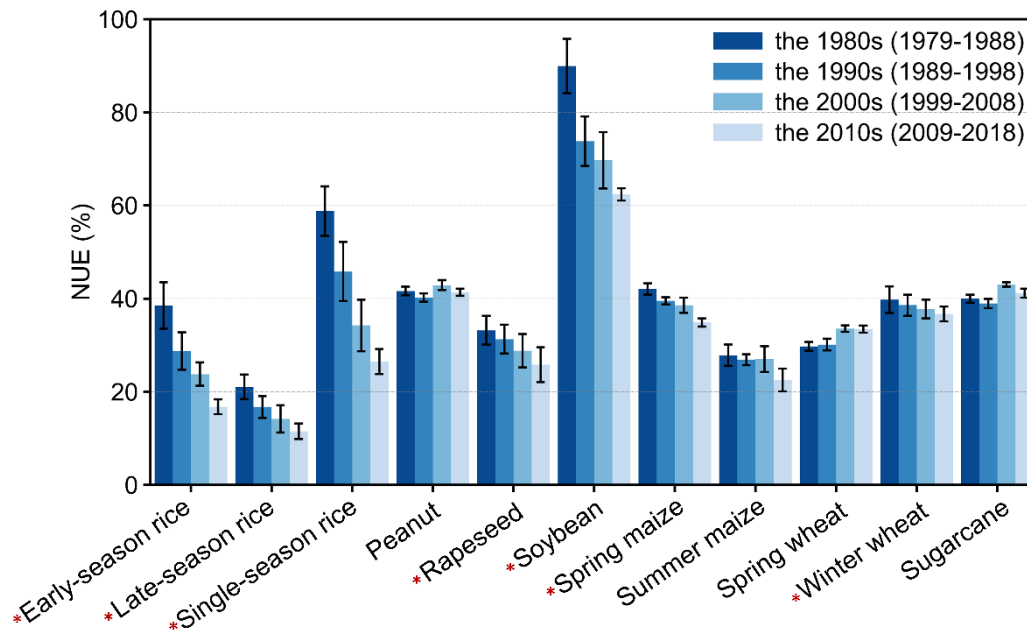
302 The average NUE for 1979 to 2018 was calculated to examine the spatial patterns of plant nitrogen  
303 uptake on the Yangtze Plain. Considerable variations were detected across the entire Yangtze Plain,  
304 with NUE values ranging from 5% to 60% (Fig. 4a). Two hotspots of high NUE were in the Hubei and  
305 Jiangsu Province (see locations in Fig.1), dominated by cultivations of single-season rice and winter  
306 wheat under the moderate levels (i.e.,  $\sim 200 \text{ kg N ha}^{-1} \text{ yr}^{-1}$ ) of fertilizer applications (Fig. S3). The NUE  
307 values also differed among different crop types for the past four decades. The largest NUE values were  
308 found for soybean ( $74.0 \% \pm 11.0 \%$ , Fig 5), while the lowest values were found for late-season rice  
309 ( $15.9\% \pm 4.3\%$ ).

310 Due to the unprecedented increase of chemical fertilizer application since the 1980s, the crop NUE on  
311 the Yangtze Plain has significantly decreased from ca. 50% in 1979 to 25% in 2018 ( $p < 0.05$ , in Fig.  
312 4b), with an overall annual change rate of  $-0.55 \% \text{ yr}^{-1}$ . Overall, regions with relatively high levels of  
313 NUE depicted a moderate or even slight increase for the past four decades, while the regions dominated  
314 low-level NUE (i.e., Hubei and Hunan provinces in Fig. 1) experienced strongly declining trends (Fig.  
315 4a&4c), as a result of the enhanced fertilizer applications. Considerable differences in magnitudes and  
316 trends of NUE were also examined among the crop types. Significant decreases (t-test,  $p < 0.05$ ) in the  
317 decadal NUEs were found for seven crop types (annotated with “\*” in Fig. 5), with the largest decrease  
318 for the double cropping of early- and late-season rice (Fig. 4c and S3). In contrast, three crop types  
319 experienced increasing trends of NUE, including peanut, spring wheat, and sugarcane (Fig. 5).



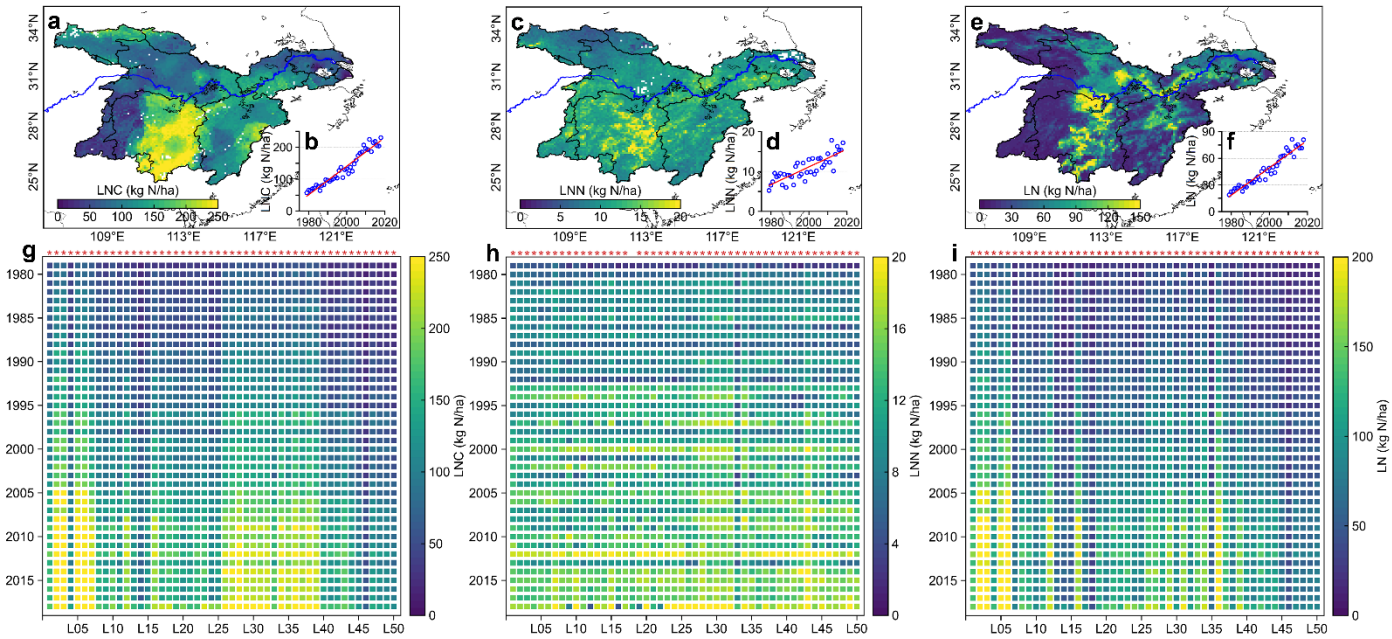
320

321 **Figure 4.** Nitrogen use efficiency (NUE) on the Yangtze Plain from 1979 to 2018. (a) Spatial  
 322 distributions of climatological NUE (1979-2018), and the inset (b) shows the long-term trends of the  
 323 area mean NUE; (c) Changes in NUE between the first (1979-1988) and the last (2009-2018) decades.



324

325 **Figure 5.** Decadal values of NUE for each crop functional type, averaged over the Yangtze Plain for  
 326 the past four decades. Significantly decreasing trends ( $p < 0.05$ ) are annotated with \* using a t-test.



327

328 **Figure 6.** Tempo-spatial patterns of leached nitrogen from cropland (LNC), natural land (LNN), and  
 329 total leached nitrogen (LN) for the period of 1979-2018. Spatial distributions of climatological (a) LNC,  
 330 (c) LNN, and (e) LN. The insets (b), (d) and (f) represent the long-term changes of mean LNC, LNN  
 331 and LN, where the red lines are the linear fitting lines between years and nitrogen leaching. Inter-annual  
 332 changes of (g) LNC, (h) LNN, and (i) LN for all examined lakes (L01-L50) from 1979 to 2018.  
 333 Statistically significantly positive trends ( $p < 0.05$ ) are annotated with ‘\*’ on top of the panel, and see  
 334 Fig. 1 for ID numbers of lakes.

### 335 3.3 Temporal and spatial patterns of nitrogen leaching for the past four decades

336 Along with the overall decreases in NUE, the leached nitrogen from both agricultural (LNC, averaged  
 337 across cropland area) and natural systems (LNN, averaged across the natural area) experienced a  
 338 statistically significant increase (t-test,  $p < 0.05$ ) over the past four decades, with the different rates (4.5  
 339  $\text{kg N ha}^{-1}\text{yr}^{-2}$  and  $0.22 \text{ kg N ha}^{-1} \text{ yr}^{-2}$  derived through the linear regression, respectively in Fig. 6b, 6d).  
 340 The increased LNC was primarily associated with increased fertilizer applications (increased 2.5 times  
 341 from 1979 to 2018), while the increased LNN was mainly linked to enhanced atmospheric deposition  
 342 (explained  $75.8\% \pm 6.8\%$  of the increases in nitrogen sources) for natural ecosystems on the Yangtze  
 343 Plain. The LNC were an order of magnitude larger than the LNN. The high levels of LNC were found

344 mainly in the Hunan Province (see Fig. 1 and Fig. 6a), with an average LNC value of  $149 \text{ kg N ha}^{-1} \text{ yr}^{-1}$   
345 <sup>1</sup>. In contrast, considerable spatial variations in LNN were revealed between the north and south parts  
346 of the Yangtze Plain (Fig. 6c).

347 To understand nitrogen sources for each corresponding lake ecosystem on the Yangtze Plain, we  
348 calculated the mean leached nitrogen (LN, averaged across the ground area) over the entire catchment  
349 of each studied lake provided by the HydroLAKES dataset (Messenger et al., 2016). The LN values  
350 ranged from  $29 \text{ kg N ha}^{-1} \text{ yr}^{-1}$  in Gehu Lake (L46 in Fig. 6i) to  $153 \text{ kg N ha}^{-1} \text{ yr}^{-1}$  in Donghu Lake (L05  
351 in Fig. 6i), indicating the considerable difference between the western lakes in the Hunan Province and  
352 the eastern lakes in the Jiangsu Province. All examined lakes experienced statistically significantly  
353 increasing trends in the LN (t-test,  $p < 0.05$ ) over the past four decades (Fig. 6i), where the agricultural  
354 activities contributed  $94 \% \pm 5 \%$  to the LN changes.

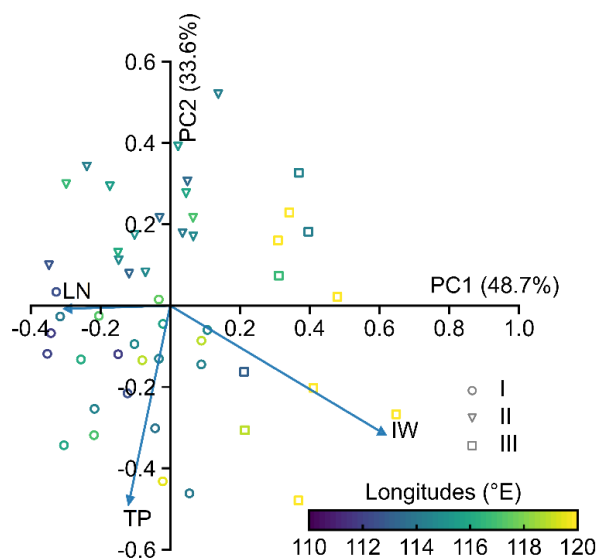
### 355 **3.4 Driving forces of terrestrial nutrient sources to eutrophication changes**

356 The leached nitrogen (LN), total phosphorus sources (TP), and industrial wastewater discharge (IW)  
357 were used to represent terrestrial nutrient sources and were further investigated in terms of their linkages  
358 to the observed PEOs. In the PCA analysis, the first two principal components (PCs) explained 48.7%  
359 and 33.6% of variations in terrestrial nutrient sources (Fig. 7), where the first PC primarily depicts  
360 positive dependence on IW but negative links with LN, and the second PC reveals negative dependences  
361 on TP and IW. All fifty lakes were clustered into three classes based on the first two PCs (Fig. 7). Lakes  
362 in class I ( $n = 22$ ) had positive loading in the direction of the total phosphorus sources, with the main  
363 coverage of the middle Yangtze Plain (i.e., Jiangxi and Anhui Province in Fig. 1), while class II cover  
364 the most of lakes ( $n = 17$ ) in the western regions (i.e., the Hunan Province and the western parts of the  
365 Hubei Province in Fig. 1). The lakes of class III ( $n = 11$ ) are primarily located on the eastern Yangtze  
366 Plain, except for two lakes (i.e., Donghu and Tangxun lakes) which located at the urban area of Wuhan  
367 City.

368 The correlations between annual anomalies of PEO and the three nutrient variables (relative to their  
369 means for 2003-2011) were examined for all three lake classes. The PEO anomalies were significantly

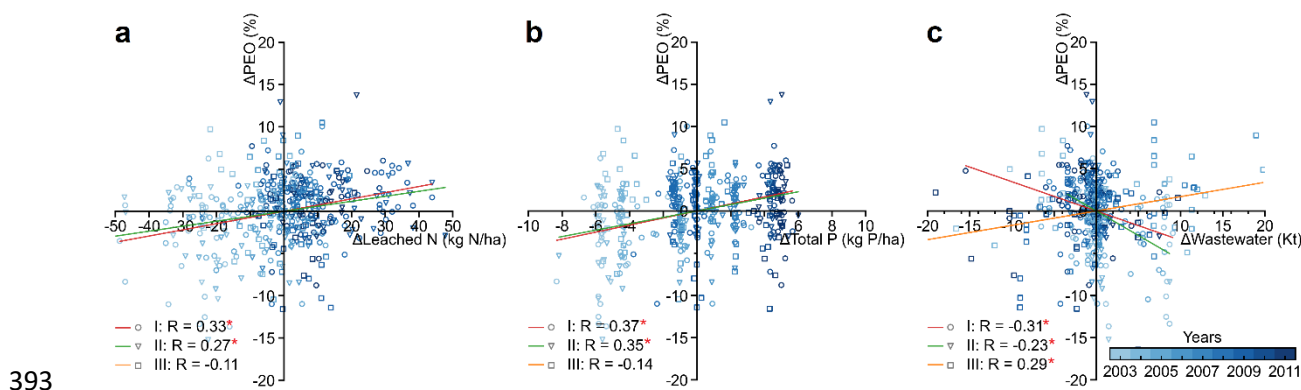


370 correlated with different nutrient variables for three lake classes, indicating spatial variations of driving  
 371 factors for eutrophication changes on the Yangtze Plain (Fig. 8). Specifically, both LN and TP  
 372 anomalies exhibited significantly positive correlations ( $p < 0.001$ ) with the PEO trends in lakes of class  
 373 I and II (Fig. 8a&b), indicating that the primary influence of agriculture-related sources to the increasing  
 374 trends of PEO. In contrast, the annual PEO dynamics in lakes of class III showed a significantly positive  
 375 correlation ( $p < 0.05$ ) with industrial wastewater discharge (Fig. 8c), meaning that the temporal trends  
 376 of annual PEO in eastern parts of the Yangtze Plain were mainly associated with industrial wastewater  
 377 discharge. Note that the significantly negative correlations between the PEO and IW anomalies were  
 378 found for class I and II (Fig. 8c), which might be mechanistically unlikely. However, lakes in class I  
 379 and II are mainly located in western and central regions, with intensive agriculture activities and high  
 380 fertilizer applications (Chen et al., 2016). Such agriculture ecosystems provided substantial nutrient  
 381 sources for eutrophication growth and development, greatly larger than available nutrient from  
 382 industrial wastewater. In addition, agriculture nutrient sources generally increased with enhanced  
 383 fertilizer applications, while industrial wastewater discharge showed overall decreasing trends (Li et al.,  
 384 2013; Lyu et al., 2016). In such cases, industrial wastewater showed negative correlation with PEO  
 385 anomalies for class I and II lakes. It was also acknowledged that such correlation between industrial  
 386 wastewater and eutrophication changes might be affected by spatial variability in examined lakes within  
 387 each class.



388

389 **Figure 7.** Loading plot of the principal component analysis (PCA) based on three nutrient-related  
 390 variables. The color of scattering points represents the distributions of lakes in longitudinal order, and  
 391 the directions of nutrient-related variables (i.e., LN leached nitrogen; TP total phosphorus sources; IW  
 392 industrial wastewater) were annotated with blue arrows.



394 **Figure 8.** Relationships between the annual anomalies of PEO and nitrogen leaching (a), total  
 395 phosphorus sources (b), and industrial wastewater discharge (c) for fifty studied lakes. The color and  
 396 symbol of scattering points represent the years and lake classes, and the colored lines (shown for  
 397 significant correlations only) are linear regressions between the annual anomalies of PEO and nutrient-  
 398 related variables for each lake class. Significant correlation coefficients are marked by the red stars “\*”.

## 399 4 Discussions

### 400 4.1 Significant decline in nitrogen use efficiency

401 The overall low mean NUE (27 %) and declining trends in NUE ( $-0.55 \text{ \% yr}^{-1}$ ) characterized agricultural  
 402 ecosystems on the Yangtze Plain for the past four decades, which are consistent with previous studies  
 403 using statistical datasets and numerical modelling (Zhang et al., 2015; Yu et al., 2019). Over-  
 404 fertilization was primarily responsible for decline in NUE from 1979 to 2018 (Shi et al., 2020; Zhang  
 405 et al., 2015). Nitrogen fertilizer applications significantly increased by 2.5 times for past four decades,  
 406 greatly exceeding the increase magnitudes in crop production (+26.3%), which potentially contributed  
 407 to markedly decreasing NUE over the Yangtze Plain. Moreover, fertilization-induced increases of crop  
 408 yield always decrease with the increase in fertilizer applications, and eventually disappear when crop  
 409 yield reaches the upper limits (Zhang et al., 2015), suggesting that high fertilization rates are more likely

410 to generate the further decline in NUE over the Yangtze Plain. Over-fertilization might potentially  
411 enhance nitrogen accumulation in soil that can be available for crop growth and development in next  
412 years (Yang et al., 2006), thereby indicating that temporally increasing fertilization rates are generally  
413 accompanied by declining NUE in agriculture ecosystems.

414 Considerable difference in NUE was examined among different crops, with the largest NUE values in  
415 soybean for the past four decades (Fig. 5) as previously-documented NUE variations from 1961 to 2011  
416 (Zhang et al., 2015). Generally, soybean has high NUEs mostly due to high protein contents (i.e., >  
417 50%) in its grains (Fabre and Planchon, 2000). With the enhanced leaf nitrogen concentrations related  
418 to its biological fixation, soybean tends to achieve a higher photosynthesis rate and delay leaf  
419 senescence (Kaschuk et al., 2010; Ma et al., 2022), both of which potentially contributed to its generally  
420 high NUE. Furthermore, double-cropping rice showed an overall lower NUE than single-season rice  
421 (Fig. 5). It has been previously reported to occur in other double-cropping systems based on field  
422 experiments, such as rice-wheat cropping (Liu et al., 2016b; Yi et al., 2015), rice-rapeseed cropping  
423 (Wang et al., 2021a), and wheat-maize cropping (Xiao et al., 2021). Indeed, fertilizer applications  
424 applied for the former crop could have accumulated nitrogen in soil that can be also taken by the latter  
425 cultivated crop for their growth and development (Shi et al., 2020). In this regard, chemical fertilizer  
426 applications for the latter crop can potentially generate the decline in its NUE.

#### 427 **4.2 Primary causes of eutrophication changes.**

428 Our study revealed that the primary nutrient causes of eutrophication changes varied with regions over  
429 the Yangtze Plain, where agricultural nutrient sources were strongly linked with eutrophication changes  
430 in western and central lakes, while industrial wastewater showed a significantly positive correlation  
431 with PEO trends in eastern lakes. Such spatial variations indicated that scientific policies and measures  
432 were required to be implemented at local scales to mitigate eutrophication issues in lake ecosystems.  
433 Separately, sustainable agriculture development should be encouraged to improve nitrogen/phosphorus  
434 use efficiency and thus reduce agriculture nutrient sources available for western and central lakes to  
435 potentially control eutrophication issues. In recent years, several agriculture practices have been  
436 recommended and implemented, such as optimal fertilization schemes and residue removal, to pursue

437 high-efficiency agriculture on the Yangtze Plain (Cui et al., 2018; Shi et al., 2020). However,  
438 smallholders were hesitant to adopt those knowledge-based practices, resulting in their poor  
439 performance on agriculture sustainability (Cai et al., 2023). By contrast, national policies about  
440 formulated fertilization was implemented in 2012, and fertilizer consumption started to decline since  
441 2014 (Deng et al., 2021), which was expected to reduce agricultural nutrient sources in western and  
442 central lakes.

443 In the eastern parts of the Yangtze Plain, policies and measures about mitigating eutrophication issues  
444 were suggested to mainly focus on the decline and treatment in industrial sewage due to its large  
445 contributions to nutrient exports delivered to lakes from the adjacent cities. The Jiangsu Province in the  
446 eastern parts of the Yangtze Plain (see the locations in Fig. 1) experienced rapid economic and industrial  
447 development since the policy of Reform and Opening-up of China since 1980s (Shen et al., 2020),  
448 suggesting that the associated industrial wastewater discharge might be enhanced and then discharge  
449 substantial nutrients to phytoplankton communities in lake ecosystems. In such cases, various national  
450 strategies and policies have been gradually implemented to promote the green growth of industries on  
451 the Yangtze Plain. Considerable efforts were made to encourage the reclamation of wastewater,  
452 investment in the advances in wastewater treatment technology and installment of municipal wastewater  
453 treatment plants (Li et al., 2013; Lyu et al., 2016). Furthermore, industrial structures were also  
454 encouraged to transform from secondary to tertiary industries under the environment-friendly targets of  
455 economic development (Huang et al., 2015). All these measures were expected to contribute to the  
456 decline in industrial sewage on the Yangtze Plain.

#### 457 **4.3 Limitations and Uncertainties**

458 Using the LPJ-GUESS model, we investigated the long-term changes and spatial variations of nitrogen  
459 dynamics (i.e., plant nitrogen uptake and nitrogen leaching) over the Yangtze Plain for the past four  
460 decades, and then examined the contributions of terrestrial nutrient sources to eutrophication changes  
461 in fifty large lakes. However, due to the lacking representation of a phosphorus cycle in the LPJ-GUESS  
462 model, we used external phosphorus fertilizer and manure application rates to represent the agricultural

463 phosphorus sources, without consideration of potential impacts from plant and soil processes.  
464 Phosphorus fertilizer applications significantly increased from 6.5 kg P ha<sup>-1</sup> in 1980 to 22.0 kg P ha<sup>-1</sup> in  
465 2014, and previous studies also reported that the overall low phosphorus use efficiency (< 40%)  
466 characterized the Yangtze Plain from 2001 to 2015 (Zheng et al., 2018), both of which were similar to  
467 nitrogen patterns on the Yangtze Plain for the past four decades. In addition, the leached nitrogen  
468 showed strong dependence on fertilizer applications ( $R^2 = 0.92$ ,  $p < 0.001$  in Fig. S4) over the Yangtze  
469 Plain for the past four decades. In this regard, we considered agricultural phosphorus sources as the  
470 potential driving force for eutrophication changes under the low levels of phosphorus use efficiency  
471 over the Yangtze Plain (Li et al., 2017; Zheng et al., 2018). Nevertheless, we also acknowledge that the  
472 use of phosphorus application data can generate uncertainties in our analysis, and thus processes related  
473 to phosphorus cycles are needed to add into LPJ-GUESS in the future to study the interactions of  
474 leached nitrogen and phosphorus on lake ecosystems.

475 Another source of uncertainty is associated with the transport processes that mediate the quantity and  
476 quality of terrestrial nutrients discharged to surface water ecosystems, as well as the impacts of  
477 aquaculture-related nutrient sources. Lateral transport rates of runoff and dissolved matter depend on  
478 soil properties, topography, and hydrological conditions over the drainage area (Solomon et al., 2015;  
479 Tang et al., 2014; Tang et al., 2018), which is required to further consider at regional scales to link to  
480 the dynamics of terrestrial nutrient exports for lake ecosystems on the Yangtze Plain. In addition,  
481 intensive and widespread freshwater aquaculture across the Yangtze Plain can contribute to accessible  
482 nutrient sources for eutrophication development and phytoplankton growth (Guo and Li, 2003; Wang  
483 et al., 2019a). Satellite observations revealed that 17 out of 50 lakes on the Yangtze Plain have  
484 established enclosure fishery nets to increase fish production (Dai et al., 2019). Consequently,  
485 substantial nutrients in fish food can directly enter aquaculture zones, promoting the contents of  
486 nitrogen and phosphorus in these lakes. These associated drivers are required to be comprehensively  
487 assessed to draw a complete picture of accessible nutrient sources for phytoplankton communities and  
488 then specify the anthropogenic impacts on water quality and eutrophication deterioration on the Yangtze  
489 Plain.

490 Uncertainties in the PEO data can originate from the uneven distributions of valid numbers of satellite  
491 observations across the fifty large lakes of the Yangtze Plain. Under the influence of observational  
492 conditions (i.e., cloud coverage and thick aerosols), the imagery with high-quality observations  
493 distributed unevenly across the different years and seasons, which potentially resulted in certain impacts  
494 on the derived annual PEOs and their temporal trends. Alternatively, the annual PEOs were calculated  
495 based on the quarterly values to minimize such uncertainties. Nevertheless, more frequent satellite  
496 observations (e.g., MODIS observations) will still be required to obtain a more accurate assessment of  
497 eutrophication changes in lake ecosystems.

## 498 **5 Conclusions**

499 We used the LPJ-GUESS model to investigate the long-term changes of nitrogen dynamics over the  
500 Yangtze Plain for the past four decades, and then examined their potential functions as the driving forces  
501 of eutrophication changes in fifty large lakes of the Yangtze Plain. Significant decreases in NUE  
502 dominated the whole Yangtze Plain, with the largest decrease in rice, soybean and rapeseed. The  
503 leached nitrogen from both cropland and natural land showed statistically significant increasing trends  
504 for all fifty examined lakes, indicating increased availability of terrestrial nitrogen sources in lake  
505 systems for the past four decades. Two classes of lakes located in the western and central parts of the  
506 Yangtze Plain showed significantly positive correlations between anomalies of PEO and agricultural  
507 nutrient sources (i.e., the leached nitrogen and total phosphorus sources), and the PEO anomalies in the  
508 remaining class (11 eastern lakes in the eastern parts of the Yangtze Plain) were positively correlated  
509 with the industrial wastewater discharge. The impacts of agricultural and industrial nutrient sources on  
510 eutrophication changes further emphasize the importance of region-specific policies and measures (i.e.,  
511 sustainable management of agricultural nitrogen and phosphorus in western and central regions, and the  
512 decline in wastewater-related nutrient discharge in eastern regions) to improve water environments.

513 *Data availability.* Data used in this study are archived by the authors and are available upon request.

514 *Author contributions.* QG, JT, LF and GS designed the framework and methodology of the study. QG  
515 drafted the first version of the manuscript and analyzed the results. QG, JT and GS performed the

516 calibration of the LPJ-GUESS model. All co-authors contributed critically to the manuscript editing  
517 and writing processes.

518 *Competing interests.* The authors declare that they have no conflict of interest.

519 *Acknowledgements.* This work was supported by the National Natural Science Foundation of China  
520 (NOs: 41971304). Qi Guan was funded by the SUSTech-UCPH Joint Program. Jing Tang was  
521 financially supported by Swedish FORMAS mobility grant (2016-01580) and MERGE Short project.  
522 Stefan Olin acknowledges support from Lund University strong research areas MERGE and eSSSENCE.  
523 We are grateful to the European Space Agency (ESA) for publishing land cover dataset and to the China  
524 Meteorological Data Service Center for providing crop distribution and yield data.

## 525 **References**

- 526 Batjes, N. H.: Harmonized soil property values for broad-scale modelling (WISE30sec) with estimates  
527 of global soil carbon stocks, *Geoderma*, 269, 61-68, 2016.
- 528 Cai, S., Zhao, X., Pittelkow, C. M., Fan, M., Zhang, X., and Yan, X.: Optimal nitrogen rate strategy for  
529 sustainable rice production in China, *Nature*, 10.1038/s41586-022-05678-x, 2023.
- 530 Chen, F., Hou, L., Liu, M., Zheng, Y., Yin, G., Lin, X., Li, X., Zong, H., Deng, F., and Gao, J.: Net  
531 anthropogenic nitrogen inputs (NANI) into the Yangtze River basin and the relationship with riverine  
532 nitrogen export, *Journal of Geophysical Research: Biogeosciences*, 121, 451-465, 2016.
- 533 Chen, Q., Huang, M., and Tang, X.: Eutrophication assessment of seasonal urban lakes in China Yangtze  
534 River Basin using Landsat 8-derived Forel-Ule index: A six-year (2013–2018) observation, *Science of  
535 the Total Environment*, 745, 135392, 2020a.
- 536 Chen, S., Ge, Q., Chu, G., Xu, C., Yan, J., Zhang, X., and Wang, D.: Seasonal differences in the rice grain  
537 yield and nitrogen use efficiency response to seedling establishment methods in the Middle and Lower  
538 reaches of the Yangtze River in China, *Field Crops Research*, 205, 157-169, 2017.
- 539 Chen, X., Wang, L., Niu, Z., Zhang, M., and Li, J.: The effects of projected climate change and extreme  
540 climate on maize and rice in the Yangtze River Basin, China, *Agricultural and Forest Meteorology*, 282,  
541 107867, 2020b.
- 542 Chen, X., Stokal, M., Kroeze, C., Supit, I., Wang, M., Ma, L., Chen, X., and Shi, X.: Modeling the  
543 contribution of crops to nitrogen pollution in the Yangtze River, *Environmental science & technology*,  
544 54, 11929-11939, 2020c.
- 545 Cui, Z., Zhang, H., Chen, X., Zhang, C., Ma, W., Huang, C., Zhang, W., Mi, G., Miao, Y., and Li, X.: Pursuing  
546 sustainable productivity with millions of smallholder farmers, *Nature*, 555, 363-366, 2018.
- 547 Dai, Y., Feng, L., Hou, X., Choi, C.-Y., Liu, J., Cai, X., Shi, L., Zhang, Y., and Gibson, L.: Policy-driven  
548 changes in enclosure fisheries of large lakes in the Yangtze Plain: Evidence from satellite imagery,  
549 *Science of the total environment*, 688, 1286-1297, 2019.
- 550 Defourny, P., Kirches, G., Brockmann, C., Boettcher, M., Peters, M., Bontemps, S., Lamarche, C., Schlerf,  
551 M., and Santoro, M.: Land cover CCI, Product User Guide Version, 2, 325, 2012.
- 552 Deng, C., Liu, L., Peng, D., Li, H., Zhao, Z., Lyu, C., and Zhang, Z.: Net anthropogenic nitrogen and  
553 phosphorus inputs in the Yangtze River economic belt: spatiotemporal dynamics, attribution analysis,  
554 and diversity management, *Journal of Hydrology*, 597, 126221, 2021.
- 555 Fabre, F. and Planchon, C.: Nitrogen nutrition, yield and protein content in soybean, *Plant Science*, 152,  
556 51-58, 2000.

557 Feng, L., Hou, X., and Zheng, Y.: Monitoring and understanding the water transparency changes of fifty  
558 large lakes on the Yangtze Plain based on long-term MODIS observations, *Remote Sensing of*  
559 *Environment*, 221, 675-686, 2019.

560 Gao, S., Xu, P., Zhou, F., Yang, H., Zheng, C., Cao, W., Tao, S., Piao, S., Zhao, Y., and Ji, X.: Quantifying  
561 nitrogen leaching response to fertilizer additions in China's cropland, *Environmental pollution*, 211,  
562 241-251, 2016.

563 Guan, Q., Feng, L., Hou, X., Schurgers, G., Zheng, Y., and Tang, J.: Eutrophication changes in fifty large  
564 lakes on the Yangtze Plain of China derived from MERIS and OLCI observations, *Remote Sensing of*  
565 *Environment*, 246, 111890, 2020.

566 Guo, L. and Li, Z.: Effects of nitrogen and phosphorus from fish cage-culture on the communities of a  
567 shallow lake in middle Yangtze River basin of China, *Aquaculture*, 226, 201-212, 2003.

568 Hartigan, J. A. and Wong, M. A.: Algorithm AS 136: A k-means clustering algorithm, *Journal of the royal*  
569 *statistical society. series c*, 28, 100-108, 1979.

570 He, J., Yang, K., Tang, W., Lu, H., Qin, J., Chen, Y., and Li, X.: The first high-resolution meteorological  
571 forcing dataset for land process studies over China, *Scientific Data*, 7, 1-11, 2020.

572 Hou, X., Feng, L., Duan, H., Chen, X., Sun, D., and Shi, K.: Fifteen-year monitoring of the turbidity  
573 dynamics in large lakes and reservoirs in the middle and lower basin of the Yangtze River, China,  
574 *Remote Sensing of Environment*, 190, 107-121, 2017.

575 Hou, X., Feng, L., Tang, J., Song, X.-P., Liu, J., Zhang, Y., Wang, J., Xu, Y., Dai, Y., and Zheng, Y.:  
576 Anthropogenic transformation of Yangtze Plain freshwater lakes: Patterns, drivers and impacts,  
577 *Remote Sensing of Environment*, 248, 111998, 2020.

578 Hu, M., Ma, R., Xiong, J., Wang, M., Cao, Z., and Xue, K.: Eutrophication state in the Eastern China  
579 based on Landsat 35-year observations, *Remote Sensing of Environment*, 277, 113057, 2022.

580 Huang, C., Zhang, M., Zou, J., Zhu, A.-x., Chen, X., Mi, Y., Wang, Y., Yang, H., and Li, Y.: Changes in land  
581 use, climate and the environment during a period of rapid economic development in Jiangsu Province,  
582 China, *Science of the Total Environment*, 536, 173-181, 2015.

583 Huang, J., Zhang, Y., Arhonditsis, G. B., Gao, J., Chen, Q., and Peng, J.: The magnitude and drivers of  
584 harmful algal blooms in China's lakes and reservoirs: A national-scale characterization, *Water Research*,  
585 181, 115902, 2020.

586 Huang, J., Zhang, Y., Arhonditsis, G. B., Gao, J., Chen, Q., Wu, N., Dong, F., and Shi, W.: How successful  
587 are the restoration efforts of China's lakes and reservoirs?, *Environment international*, 123, 96-103,  
588 2019.

589 Huang, M., Shan, S., Zhou, X., Chen, J., Cao, F., Jiang, L., and Zou, Y.: Leaf photosynthetic performance  
590 related to higher radiation use efficiency and grain yield in hybrid rice, *Field Crops Research*, 193, 87-  
591 93, 2016.

592 Kaschuk, G., Hungria, M., Leffelaar, P., Giller, K., and Kuyper, T.: Differences in photosynthetic  
593 behaviour and leaf senescence of soybean (*Glycine max* [L.] Merrill) dependent on N<sub>2</sub> fixation or  
594 nitrate supply, *Plant Biology*, 12, 60-69, 2010.

595 Lamarque, J. F., Dentener, F., McConnell, J., Ro, C. U., Shaw, M., Vet, R., Bergmann, D., Cameron-Smith,  
596 P., Dalsoren, S., and Doherty, R.: Multi-model mean nitrogen and sulfur deposition from the  
597 Atmospheric Chemistry and Climate Model Intercomparison Project (ACCMIP): evaluation of historical  
598 and projected future changes, *Atmospheric Chemistry and Physics*, 13, 7997-8018, 2013.

599 Li, A. A., Stokal, M. M., Bai, Z. Z., Kroeze, C. C., Ma, L. L., and Zhang, F. F.: Modelling reduced coastal  
600 eutrophication with increased crop yields in Chinese agriculture, *Soil Research*, 55, 506-517, 2017.

601 Li, S., Liu, C., Sun, P., and Ni, T.: Response of cyanobacterial bloom risk to nitrogen and phosphorus  
602 concentrations in large shallow lakes determined through geographical detector: A case study of Taihu  
603 Lake, China, *Science of The Total Environment*, 816, 151617, 2022.

604 Li, X. and Xiao, J.: A global, 0.05-degree product of solar-induced chlorophyll fluorescence derived from  
605 OCO-2, MODIS, and reanalysis data, *Remote Sensing*, 11, 517, 2019.

606 Li, Y., Luo, X., Huang, X., Wang, D., and Zhang, W.: Life cycle assessment of a municipal wastewater  
607 treatment plant: a case study in Suzhou, China, *Journal of cleaner production*, 57, 221-227, 2013.



608 Lindeskog, M., Arneth, A., Bondeau, A., Waha, K., Seaquist, J., Olin, S., and Smith, B.: Implications of  
609 accounting for land use in simulations of ecosystem carbon cycling in Africa, *Earth System Dynamics*,  
610 4, 385-407, 2013.

611 Liu, X., Wang, H., Zhou, J., Hu, F., Zhu, D., Chen, Z., and Liu, Y.: Effect of N fertilization pattern on rice  
612 yield, N use efficiency and fertilizer–N fate in the Yangtze River Basin, China, *PloS one*, 11, e0166002,  
613 2016a.

614 Liu, X., Xu, S., Zhang, J., Ding, Y., Li, G., Wang, S., Liu, Z., Tang, S., Ding, C., and Chen, L.: Effect of  
615 continuous reduction of nitrogen application to a rice-wheat rotation system in the middle-lower  
616 Yangtze River region (2013–2015), *Field Crops Research*, 196, 348-356, 2016b.

617 Lu, C. and Tian, H.: Global nitrogen and phosphorus fertilizer use for agriculture production in the past  
618 half century: shifted hot spots and nutrient imbalance, *Earth System Science Data*, 9, 181-192, 2017.

619 Lyu, S., Chen, W., Zhang, W., Fan, Y., and Jiao, W.: Wastewater reclamation and reuse in China:  
620 opportunities and challenges, *Journal of Environmental Sciences*, 39, 86-96, 2016.

621 Ma, J., Olin, S., Anthoni, P., Rabin, S. S., Bayer, A. D., Nyawira, S. S., and Arneth, A.: Modeling symbiotic  
622 biological nitrogen fixation in grain legumes globally with LPJ-GUESS (v4. 0, r10285), *Geoscientific*  
623 *Model Development*, 15, 815-839, 2022.

624 Messenger, M. L., Lehner, B., Grill, G., Nedeva, I., and Schmitt, O.: Estimating the volume and age of  
625 water stored in global lakes using a geo-statistical approach, *Nature communications*, 7, 13603, 2016.

626 Olin, S., Schurgers, G., Lindeskog, M., Wårlind, D., Smith, B., Bodin, P., Holmér, J., and Arneth, A.:  
627 Modelling the response of yields and tissue C: N to changes in atmospheric CO<sub>2</sub> and N management  
628 in the main wheat regions of western Europe, *Biogeosciences*, 12, 2489-2515, 2015a.

629 Olin, S., Lindeskog, M., Pugh, T., Schurgers, G., Wårlind, D., Mishurov, M., Zaehle, S., Stocker, B. D.,  
630 Smith, B., and Arneth, A.: Soil carbon management in large-scale Earth system modelling: implications  
631 for crop yields and nitrogen leaching, *Earth System Dynamics*, 6, 745-768, 2015b.

632 Parton, W., Scurlock, J., Ojima, D., Gilmanov, T., Scholes, R., Schimel, D. S., Kirchner, T., Menaut, J. C.,  
633 Seastedt, T., and Garcia Moya, E.: Observations and modeling of biomass and soil organic matter  
634 dynamics for the grassland biome worldwide, *Global biogeochemical cycles*, 7, 785-809, 1993.

635 Parton, W. J., Hanson, P. J., Swanston, C., Torn, M., Trumbore, S. E., Riley, W., and Kelly, R.: ForCent  
636 model development and testing using the Enriched Background Isotope Study experiment, *Journal of*  
637 *Geophysical Research: Biogeosciences*, 115, 2010.

638 Piao, S., Ciais, P., Huang, Y., Shen, Z., Peng, S., Li, J., Zhou, L., Liu, H., Ma, Y., and Ding, Y.: The impacts  
639 of climate change on water resources and agriculture in China, *Nature*, 467, 43-51, 2010.

640 Qin, B., Paerl, H. W., Brookes, J. D., Liu, J., Jeppesen, E., Zhu, G., Zhang, Y., Xu, H., Shi, K., and Deng, J.:  
641 Why Lake Taihu continues to be plagued with cyanobacterial blooms through 10 years (2007–2017)  
642 efforts, *Science Bulletin*, 64, 2019.

643 Qu, J. and Fan, M.: The current state of water quality and technology development for water pollution  
644 control in China, *Critical reviews in environmental science & technology*, 40, 519-560, 2010.

645 Shen, F., Yang, L., He, X., Zhou, C., and Adams, J. M.: Understanding the spatial–temporal variation of  
646 human footprint in Jiangsu Province, China, its anthropogenic and natural drivers and potential  
647 implications, *Scientific reports*, 10, 1-12, 2020.

648 Shi, X., Hu, K., Batchelor, W. D., Liang, H., Wu, Y., Wang, Q., Fu, J., Cui, X., and Zhou, F.: Exploring  
649 optimal nitrogen management strategies to mitigate nitrogen losses from paddy soil in the middle  
650 reaches of the Yangtze River, *Agricultural Water Management*, 228, 105877, 2020.

651 Sitch, S., Smith, B., Prentice, I. C., Arneth, A., Bondeau, A., Cramer, W., Kaplan, J. O., Levis, S., Lucht,  
652 W., and Sykes, M. T.: Evaluation of ecosystem dynamics, plant geography and terrestrial carbon cycling  
653 in the LPJ dynamic global vegetation model, *Global change biology*, 9, 161-185, 2003.

654 Smith, B., Wårlind, D., Arneth, A., Hickler, T., Leadley, P., Siltberg, J., and Zaehle, S.: Implications of  
655 incorporating N cycling and N limitations on primary production in an individual-based dynamic  
656 vegetation model, *Biogeosciences*, 11, 2027-2054, 2014.

657 Solomon, C. T., Jones, S. E., Weidel, B. C., Buffam, I., Fork, M. L., Karlsson, J., Larsen, S., Lennon, J. T.,  
658 Read, J. S., and Sadro, S.: Ecosystem consequences of changing inputs of terrestrial dissolved organic  
659 matter to lakes: current knowledge and future challenges, *Ecosystems*, 18, 376-389, 2015.

660 Tang, J., Pilesjö, P., Miller, P. A., Persson, A., Yang, Z., Hanna, E., and Callaghan, T. V.: Incorporating  
661 topographic indices into dynamic ecosystem modelling using LPJ-GUESS, *Ecohydrology*, 7, 1147-1162,  
662 2014.

663 Tang, J., Yurova, A. Y., Schurgers, G., Miller, P. A., Olin, S., Smith, B., Siewert, M. B., Olefeldt, D., Pilesjö,  
664 P., and Poska, A.: Drivers of dissolved organic carbon export in a subarctic catchment: Importance of  
665 microbial decomposition, sorption-desorption, peatland and lateral flow, *Science of the Total  
666 Environment*, 622, 260-274, 2018.

667 Tilman, D., Balzer, C., Hill, J., and Befort, B. L.: Global food demand and the sustainable intensification  
668 of agriculture, *Proceedings of the national academy of sciences*, 108, 20260-20264, 2011.

669 Tong, Y., Xiwen, X., Miao, Q., Jingjing, S., Yiyang, Z., Wei, Z., Mengzhu, W., Xuejun, W., and Yang, Z.:  
670 Lake warming intensifies the seasonal pattern of internal nutrient cycling in the eutrophic lake and  
671 potential impacts on algal blooms, *Water Research*, 188, 116570, 2021.

672 Tong, Y., Zhang, W., Wang, X., Couture, R.-M., Larssen, T., Zhao, Y., Li, J., Liang, H., Liu, X., and Bu, X.:  
673 Decline in Chinese lake phosphorus concentration accompanied by shift in sources since 2006, *Nature  
674 Geoscience*, 10, 507-511, 2017.

675 Wang, C., Yan, Z., Wang, Z., Batool, M., El-Badri, A. M., Bai, F., Li, Z., Wang, B., Zhou, G., and Kuai, J.:  
676 Subsoil tillage promotes root and shoot growth of rapeseed in paddy fields and dryland in Yangtze  
677 River Basin soils, *European Journal of Agronomy*, 130, 126351, 2021a.

678 Wang, D., Zhang, S., Zhang, H., and Lin, S.: Omics study of harmful algal blooms in China: Current status,  
679 challenges, and future perspectives, *Harmful algae*, 107, 102079, 2021b.

680 Wang, J., Beusen, A. H., Liu, X., and Bouwman, A. F.: Aquaculture production is a large, spatially  
681 concentrated source of nutrients in Chinese freshwater and coastal seas, *Environmental science &  
682 technology*, 54, 1464-1474, 2019a.

683 Wang, L. and Davis, J.: Can China Feed its People into the Next Millennium? Projections for China's  
684 grain supply and demand to 2010, *International Review of Applied Economics*, 12, 53-67, 1998.

685 Wang, M., Janssen, A. B., Bazin, J., Stokal, M., Ma, L., and Kroeze, C.: Accounting for interactions  
686 between Sustainable Development Goals is essential for water pollution control in China, *Nature  
687 communications*, 13, 1-13, 2022.

688 Wang, M., Stokal, M., Burek, P., Kroeze, C., Ma, L., and Janssen, A. B.: Excess nutrient loads to Lake  
689 Taihu: Opportunities for nutrient reduction, *Science of the Total Environment*, 664, 865-873, 2019b.

690 Xiao, Q., Dong, Z., Han, Y., Hu, L., Hu, D., and Zhu, B.: Impact of soil thickness on productivity and  
691 nitrate leaching from sloping cropland in the upper Yangtze River Basin, *Agriculture, Ecosystems &  
692 Environment*, 311, 107266, 2021.

693 Xu, H., Paerl, H., Qin, B., Zhu, G., Hall, N., and Wu, Y.: Determining critical nutrient thresholds needed  
694 to control harmful cyanobacterial blooms in eutrophic Lake Taihu, China, *Environmental science &  
695 technology*, 49, 1051-1059, 2015.

696 Xu, X., Hu, H., Tan, Y., Yang, G., Zhu, P., and Jiang, B.: Quantifying the impacts of climate variability and  
697 human interventions on crop production and food security in the Yangtze River Basin, China, 1990–  
698 2015, *Science of the Total Environment*, 665, 379-389, 2019.

699 Yang, S.-M., Malhi, S. S., Song, J.-R., Xiong, Y.-C., Yue, W.-Y., Lu, L. L., Wang, J.-G., and Guo, T.-W.: Crop  
700 yield, nitrogen uptake and nitrate-nitrogen accumulation in soil as affected by 23 annual applications  
701 of fertilizer and manure in the rainfed region of Northwestern China, *Nutrient Cycling in  
702 Agroecosystems*, 76, 81-94, 2006.

703 Yi, Q., He, P., Zhang, X., Yang, L., and Xiong, G.: Optimizing fertilizer nitrogen for winter wheat  
704 production in Yangtze River region in China, *Journal of Plant Nutrition*, 38, 1639-1655, 2015.

705 Yu, C., Huang, X., Chen, H., Godfray, H. C. J., Wright, J. S., Hall, J. W., Gong, P., Ni, S., Qiao, S., and  
706 Huang, G.: Managing nitrogen to restore water quality in China, *Nature*, 567, 516-520, 2019.

707 Yu, Q., Wang, F., Li, X., Yan, W., Li, Y., and Lv, S.: Tracking nitrate sources in the Chaohu Lake, China,  
708 using the nitrogen and oxygen isotopic approach, *Environmental Science and Pollution Research*, 25,  
709 19518-19529, 2018.

710 Zhang, B., Tian, H., Lu, C., Dangal, S. R., Yang, J., and Pan, S.: Global manure nitrogen production and  
711 application in cropland during 1860–2014: a 5 arcmin gridded global dataset for Earth system  
712 modeling, *Earth System Science Data*, 9, 667-678, 2017.

713 Zhang, C., Ju, X., Powlson, D., Oenema, O., and Smith, P.: Nitrogen surplus benchmarks for controlling  
714 N pollution in the main cropping systems of China, *Environmental science & technology*, 53, 6678-  
715 6687, 2019.

716 Zhang, M., Shi, X., Yang, Z., Yu, Y., Shi, L., and Qin, B.: Long-term dynamics and drivers of phytoplankton  
717 biomass in eutrophic Lake Taihu, *Science of the Total Environment*, 645, 876-886, 2018.

718 Zhang, N., Gao, Z., Wang, X., and Chen, Y.: Modeling the impact of urbanization on the local and  
719 regional climate in Yangtze River Delta, China, *Theoretical and applied climatology*, 102, 331-342, 2010.

720 Zhang, X., Davidson, E. A., Mauzerall, D. L., Searchinger, T. D., Dumas, P., and Shen, Y.: Managing  
721 nitrogen for sustainable development, *Nature*, 528, 51-59, 2015.

722 Zhang, Y., Sun, M., Yang, R., Li, X., Zhang, L., and Li, M.: Decoupling water environment pressures from  
723 economic growth in the Yangtze River Economic Belt, China, *Ecological Indicators*, 122, 107314, 2021.

724 Zhao, J., Luo, Q., Deng, H., and Yan, Y.: Opportunities and challenges of sustainable agricultural  
725 development in China, *Philosophical Transactions of the Royal Society B: Biological Sciences*, 363, 893-  
726 904, 2008.

727 Zhao, S., Chen, Y., Gu, X., Zheng, M., Fan, Z., Luo, D., Luo, K., and Liu, B.: Spatiotemporal variation  
728 characteristics of livestock manure nutrient in the soil environment of the Yangtze River Delta from  
729 1980 to 2018, *Scientific Reports*, 12, 1-17, 2022.

730 Zheng, J., Wang, W., Cao, X., Feng, X., Xing, W., Ding, Y., Dong, Q., and Shao, Q.: Responses of  
731 phosphorus use efficiency to human interference and climate change in the middle and lower reaches  
732 of the Yangtze River: historical simulation and future projections, *Journal of Cleaner Production*, 201,  
733 403-415, 2018.

734 Zhu, Z., Bi, J., Pan, Y., Ganguly, S., Anav, A., Xu, L., Samanta, A., Piao, S., Nemani, R. R., and Myneni, R.  
735 B.: Global data sets of vegetation leaf area index (LAI) 3g and fraction of photosynthetically active  
736 radiation (FPAR) 3g derived from global inventory modeling and mapping studies (GIMMS) normalized  
737 difference vegetation index (NDVI3g) for the period 1981 to 2011, *Remote sensing*, 5, 927-948, 2013.

738